

Segment Number and Axial Identity in a Segmentation Clock Period Mutant

Christian Schröter¹ and Andrew C. Oates^{1,*}

¹Max Planck Institute of Molecular Cell Biology and Genetics, Pfotenhauerstraße 108, D-01307 Dresden, Germany

Summary

A species-specific number of segments is a hallmark of the vertebrate body plan. The first segmental structures in the vertebrate embryo are the somites, which bud sequentially from the growing presomitic mesoderm (PSM). The Clock and Wavefront model for somitogenesis [1, 2] proposes that the total number of somites is determined by the period of an oscillator or clock operating in the PSM and the total duration of PSM growth. Furthermore, the number of oscillations of the segmentation clock has been suggested to regulate the regional identity of segments along the body axis [3, 4]. Here we test these two ideas in a zebrafish mutant in which the segmentation clock is specifically slowed. This reduces segment number as predicted, but *hox* gene expression and posterior anatomical markers align with lower segmental counts in mutants compared to the wild-type, arguing against an instructive role of the segmentation clock in determining axial identities. Our data therefore suggest that precise control of segmentation clock period in relation to axial growth ensures a species-specific segment number and that during evolution modulating the clock's period through genetic mutations may have been a relevant way to vary segment number independently of axial regionalization.

Results and Discussion

Slowing the Segmentation Clock Increases Segment Size and Reduces Segment Number

Hairy and enhancer of split related (hes/her) genes encode transcriptional repressor proteins and are important components of the zebrafish segmentation clock [5], but whether they regulate the period of the clock is not known. In this report we investigate the role of one member of this group, the *hes6* gene (formerly *her 13.2* [6]), for its role in period setting by using a retroviral insertion mutant [7]. The proviral insertion in the 3' end of the first exon of the gene introduces a stop codon before the conserved bHLH domain, which mediates dimerization and DNA binding in this protein family (Figures S1A and S1B, available online). In addition, the insertion strongly reduces expression of mature *hes6* mRNA (Figures S1C and S1D). Most of the *hes6* mutant embryos segment normally (Figure 1A, lower left, and Table S1), and segmentation defects in mutants occur with a lower frequency compared to situations in which *hes6* function is inhibited by injection of antisense morpholino oligonucleotides (MOs) (Figure S1E, Table S1). To test whether the retroviral insertion results in a strong loss of *hes6* function, we injected *her1*-targeted MOs into the mutants. This resulted in disruption of segmentation

along the entire axis (Figure 1A, lower left), a phenocopy of the effects of joint MO-knockdown of *hes6* and *her 1* [8]. Taken together, these results indicate that the genetic *hes6* lesion investigated here acts as a strongly hypomorphic allele. We next asked whether this mutation might influence the period of the segmentation clock.

Somitogenesis period, i.e., the time taken to form one bilateral pair of somites, is the morphological output of the segmentation clock's period and can be documented precisely with multiple-embryo time-lapse imaging [9]. All the following experiments were carried out with embryos from incrosses of heterozygous carriers of the *hes6* mutation, which were only genotyped after analysis, thereby eliminating potential observer bias. When we filmed homozygous *hes6* mutant embryos alongside their wild-type siblings, we found that somitogenesis period in the mutants was increased along the entire axis (Figure 1B, see also Movie S1). In the embryo trunk, somitogenesis period is constant, and its value can be estimated by a linear fit to the data points up to somite 18 [9]. We find that trunk somitogenesis period is lengthened by $6.5\% \pm 1.2\%$ (mean \pm 95% confidence interval [CI], $n = 29$) in *hes6* mutant compared to wild-type embryos (Figure 1C). Nevertheless, the total time of segmentation, from formation of the second somite boundary to the last visible boundary, is unchanged between wild-type and *hes6* mutant embryos (Figure 1D, see also Movie S1). Consequently, the total number of somites observed in live *hes6* mutant embryos was reduced compared to their wild-type siblings (Table 1 and Movie S1). Thus, the dynamics, but not the total duration of somitogenesis, is altered in *hes6* mutant embryos, indicating that *hes6* might be involved in setting the period of the segmentation clock.

To rule out the possibility that the slowed somitogenesis period in the *hes6* mutant reflects an alteration of general developmental dynamics, we investigated axial elongation and PSM differentiation in the *hes6* mutant. We first measured embryo length at different developmental stages from time-lapse movies (Figure 2A). Throughout trunk somitogenesis, *hes6* mutants were of the same axial length as their wild-type siblings (Figure 2B), indicating that *hes6* mutants do not differ from wild-type embryos with respect to overall size or growth. *hes6* has been implicated in positioning the wavefront where somites become determined within the PSM [6]. It is therefore possible that loss of *hes6* function specifically affects differentiation in the PSM. To rule this out, we measured PSM length from time-lapse movies and found no change between wild-type and *hes6* mutants at three different time points (Figure 2C). In addition, we determined PSM length and wavefront position in fixed PSMs at the ten-somite stage by double staining with the segment marker *myoD* and the wavefront marker *mespb* (Figure 2D). The length of the PSM and the extent of the *mespb* domain within it were again indistinguishable between wild-type and *hes6* mutants (Figure 2E). These data argue against a role of *hes6* in determining growth and differentiation in the PSM and suggest that the observed slowing of somitogenesis period in the *hes6* mutant is due to a specifically slowed segmentation clock. If this were the case, then according to the Clock and Wavefront model

*Correspondence: oates@mpi-cbg.de

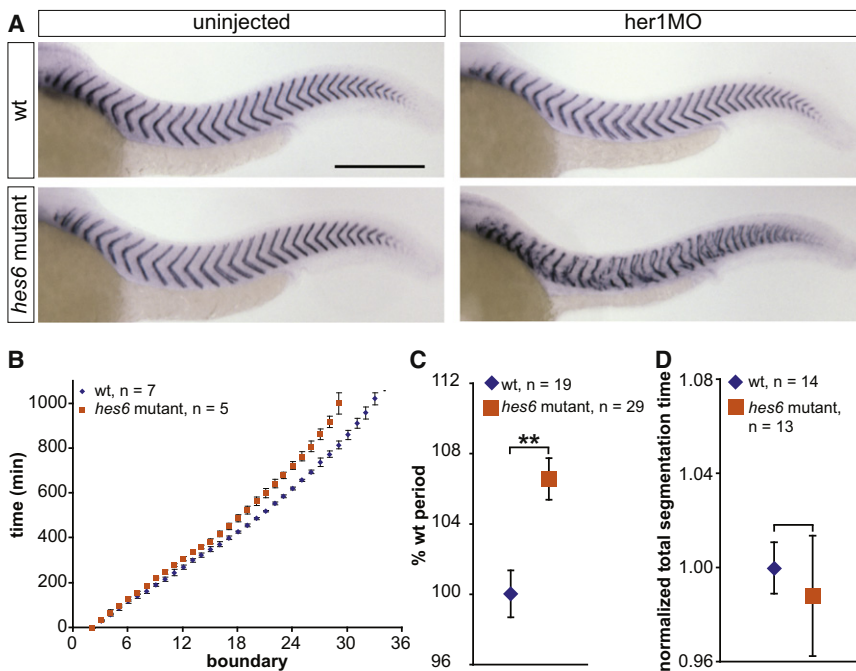


Figure 1. Mutating *hes6* Slows Somitogenesis Period

(A) Uninjected and *her1MO*-injected wild-type and *hes6* mutant embryos were stained with a *cb1045* riboprobe to analyze segmentation. Wild-type (upper left), *hes6* mutant (lower left), and *her1MO*-injected wild-type embryos (upper right) segment grossly normally, but injecting *her1MO* into *hes6* mutants disrupts segmentation (lower right). For segmentation phenotypes of *hes6* morphants, see also Figure S1 and Table S1. The scale bar represents 0.3 mm.

(B) To determine somitogenesis period along the entire axis, embryos were anesthetized with 0.02% tricaine and filmed in a multiple-embryo time-lapse array. Formation times of somite boundaries were read from the movies and normalized to the formation time of the second somite boundary for each individual. Data points show mean formation times \pm standard deviation for each somite and genotype. Somitogenesis period is increased in *hes6* mutant embryos along the entire axis, and *hes6* mutants stop somitogenesis with a smaller number of segments. One representative experiment out of three independent trials is shown.

(C) Trunk somitogenesis period was estimated from a linear fit to the data points corresponding to somites two through 18 in the somite number

versus time plot. Data were pooled from three independent experiments by normalizing wild-type period to 100%. *hes6* mutants segment \sim 6.5% slower than their wild-type siblings.

(D) Total segmentation time was calculated from time-lapse movies as the time span between formation of the second and the last visible somite boundary. Data are pooled from three independent experiments by normalizing the mean segmentation time of wild-type embryos to 1. Wild-type and *hes6* mutant embryos segment for the same total amount of time.

Data in (C) and (D) are displayed as mean \pm 95% CI. ** $p \leq 0.001$, Student's *t* test.

[1] embryonic segments should be lengthened in proportion to the slowing of the clock. We tested this prediction for somites two to four by measuring their anteroposterior length along the notochord (Figure 2F, red lines). Segment length in the *hes6* mutants was increased in good quantitative agreement with the longer somitogenesis period (Figure 2G). Together, these data indicate that the segmentation clock is specifically slowed independent of axial elongation in *hes6* mutant embryos. We conclude that the dynamics of these two processes have been dissociated.

Such dissociation is expected to change the total number of embryonic segments, and examination of live embryos from time-lapse recordings (Figure 1B, Table 1) indicated that this was the case. To test whether these differences could also

be observed in fixed specimens at later stages of development, we first grew embryos to 48 hr postfertilization (hpf), which is approximately 18 hr after the end of somitogenesis, and used the myotome boundary marker *cb1045* to count embryonic segment number (Figure 3A). At this stage, we counted approximately 2.5 segments more in wild-type embryos compared to *hes6* mutants (Table 1). This difference of approximately 9% is in reasonable quantitative agreement with the changes in somitogenesis period and somite length described above. Therefore, the slowing of the segmentation oscillator upon mutation of *hes6* translates into a reduction of embryonic segment number. This reduction was not further enhanced by MO-mediated knockdown of *hes6* in the insertion mutant, once again emphasizing that the retroviral insertion

Table 1. *hes6* Mutants Have a Reduced Number of Embryonic and Adult Segments, and the Reduction in Segment Number Is Distributed along the Axis

Feature	Wild-Type	<i>hes6</i> Mutant
Number of myotomes (live embryos)	33.4 \pm 0.3 (n = 14)	29.7 \pm 0.5 (n = 13)
Number of myotomes (48 hpf, <i>cb1045</i>)	31.6 \pm 0.2 (n = 33)	29.2 \pm 0.2 (n = 26)
Level of proctodeum	17.5 \pm 0.2 (n = 16)	16.1 \pm 0.1 (n = 12)
Anterior boundary of <i>hoxd12a</i> expression	18.9 \pm 0.6 (n = 11)	17.4 \pm 0.3 (n = 14)
Number of vertebrae	26.3 \pm 0.1 (n = 43)	24.4 \pm 0.2 (n = 42)
Number of rib-bearing vertebrae	9.5 \pm 0.2 (n = 43)	9.0 \pm 0.1 (n = 42)
Anterior insertion site of dorsal fin	9.0 \pm 0.2 (n = 38)	8.4 \pm 0.2 (n = 33)
Anterior insertion site of anal fin	10.8 \pm 0.1 (n = 38)	10.2 \pm 0.1 (n = 38)

Vertebrae number, rib number, and the insertion sites of the dorsal and anal fins were counted in adult fish between 2 and 10 months of age stained with alizarin red S. Myotome number was scored in live embryos at 36 hpf or in 48 hpf embryos stained with the myotome marker *cb1045*; in a subset of these embryos, the level of the proctodeum was determined by costaining for *evx1*. The anterior position of *hoxd12a* expression was determined in 25 hpf embryos stained for *hoxd12a* and *cb1045* expression. Myotome number, the position of the proctodeum, and the anterior boundary of *hoxd12a* expression were scored by an observer blind to the embryos' genotype, and specimens were genotyped only after phenotypic analysis. Counts are given as mean \pm 95% CI. All differences are highly significant as judged by Student's *t* test ($p \leq 0.001$).

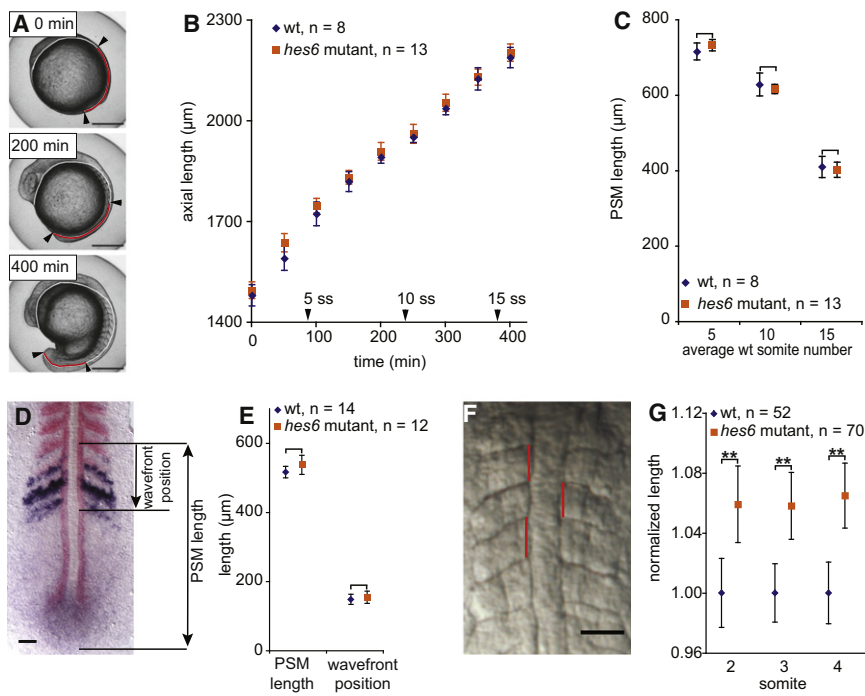


Figure 2. Unchanged Axial Elongation and Longer Somites in *hes6* Mutant Embryos

(A) Total axial length was measured from stills of time-lapse movies by drawing a line (red plus white) from the anterior to the posterior end of the embryo, following the yolk and the dorsal aspect of the paraxial mesoderm. PSM length was measured along the same line (red part) as the distance between the most recently formed somite boundary (arrowhead) and the posterior end of the mesoderm (arrowhead). Three representative stages are shown. The scale bar represents 0.3 mm.

(B) Axial length as measured in (A) is indistinguishable between wild-type and *hes6* mutants throughout trunk somitogenesis. Arrowheads on the x axis indicate when wild-type embryos reached the five-, ten-, and 15-somite stage.

(C) PSM length measured as in (A) (red line) is indistinguishable between wild-type and *hes6* mutants at three stages during trunk somitogenesis. Measurements were taken at simultaneous time points in all samples; the x axis label indicates average number of somites in wild-type embryos at the respective time point.

(D) PSM length and wavefront position measurement from a fixed PSM stained with *myoD* (red) to label formed somites and *mespb* (dark blue) to indicate the wavefront position. Embryo is at the ten-somite stage, flat mount, anterior to the top. The scale bar represents 50 μm .

(E) PSM length and distance of the wavefront from the most recently formed somite boundary as indicated in (D) are indistinguishable between wild-type and *hes6* mutant embryos. Genotypes were determined by the presence or absence of *hes6* *in situ* signal (blue staining in the tailbud in D).

One representative experiment from three independent trials is shown in (B) and (C) and from two independent trials in (E). In no case was a difference between wild-type and mutant embryos observed.

(F) Anteroposterior length of somites two to four was measured by drawing a straight line (red) connecting the contact points of the rostral and caudal somite boundaries with the notochord. The scale bar represents 50 μm .

(G) Mean anteroposterior length of somites two to four. Data are pooled from four independent experiments by normalizing mean length of wild-type somites to 1. Somites in *hes6* mutants are approximately 6%–7% longer than in their wild-type siblings.

Data in (B), (C), (E), and (G) are given as mean \pm 95% CI; ** $p \leq 0.001$, Student's t test.

creates a strongly hypomorphic allele (Table S2). Next, we wanted to know whether mutation of *hes6* also affected the anatomy of the adult fish. We performed skeletal stains of wild-type and *hes6* mutants and counted vertebral number from the first rib-bearing vertebra to the first caudal vertebra contacting the tail fin (Figure 3B). This count was reduced to 24 or 25 vertebrae in *hes6* mutants compared to 26 or 27 in wild-type fish (Figure 3B and Table 1). This rules out the existence of mechanisms that correct segment number later in development and shows that dissociation of segmentation oscillator period and axial outgrowth dynamics provides a means to vary adult segment number.

Based on phylogenetic studies, it has been proposed that dissociation [10, 11] of the developmental modules responsible for segmentation clock period and axial elongation has occurred repeatedly in evolution, generating novel body plans and fostering vertebrate radiation [12, 13]. More recently, Gomez et al. [14] investigated somitogenesis in a panel of model vertebrates and, using a mathematical model of tissue growth, concluded that part of the difference in their segment number is due to changes in the ratio of segmentation oscillator period and axial growth rate. However, these phylogenetic and comparative studies are limited to assessing the ratio between growth and segmentation oscillator period, because both parameters have changed when comparing between evolutionarily distant species. The present work provides the first direct experimental evidence for one of the elementary evolutionary transitions implicit in the proposed phylogenetic

scenarios by showing that the segmentation clock can be slowed independently from axial growth within a single species.

It is possible that *hes6* constitutes a molecularly hard-wired link between the dynamics of general growth and the segmentation clock period, a link that is lost in the mutant. *hes6* is a transcriptional target of fibroblast growth factor (FGF) signaling [6], and FGF has well-known roles in axial elongation of vertebrate embryos [15]. Conceivably, *hes6* may transduce FGF signaling activity and regulate clock period accordingly, thereby coupling the dynamics of both developmental modules. Alternatively, it is possible that these modules are not hard-wired and that *hes6* is just a component of the clock. Although the data presented here do not let us distinguish between these possibilities, it is clear that in either case *hes6* acts as a regulator of segmentation clock period. Because *hes6* has well-known roles in transcriptional regulation [6, 16], the data in this report provide the first experimental evidence for the idea that the pacemaking mechanism of the segmentation clock is transcriptional in nature [17], although other mechanisms cannot be ruled out.

Determination of Axial Identity Is Independent of Segment Number

Although initially very similar in morphology, segments differentiate into diverse structures depending on their axial position. The expression of *Hox* genes is one of the first molecular determinants of this region-specific differentiation [18]. Some

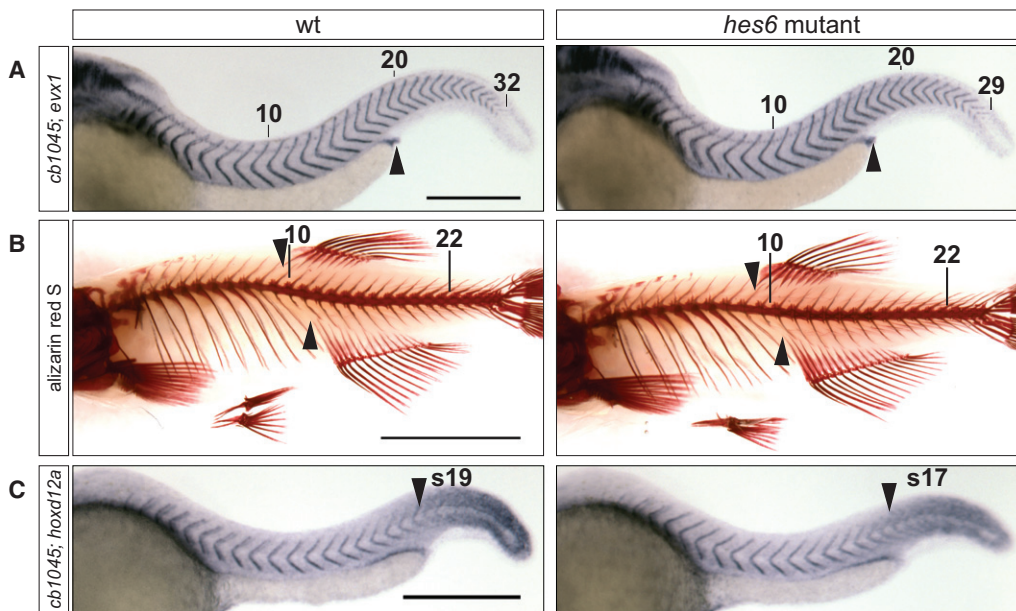


Figure 3. *hes6* Mutants Have a Reduced Number of Embryonic and Adult Segments, and the Change in Segment Number Is Distributed across Axial Regions

(A) Embryos at 48 hpf were stained with the myotome boundary marker *cb1045* and *evx1*, which labels the proctodeum (arrowhead). *hes6* mutants have fewer myotomes than their wild-type siblings, and their proctodeum aligns with the 16th segment instead of the 17th or 18th as in the wild-type. The tenth, 20th, and last segment are indicated. The scale bar represents 0.3 mm.

(B) Skeletal stains of 2-month-old wild-type and *hes6* mutant fish. The mutant has fewer vertebrae and ribs but an otherwise normal morphology of the vertebral column. The anterior insertion sites of the anal and dorsal fin (arrowheads) align with a higher vertebral number in wild-type compared to *hes6* mutant fish. The 10th and 22nd vertebrae are indicated. The scale bar represents 0.5 cm.

(C) Embryos at 25 hpf were costained for *cb1045* and *hoxd12a* expression. The anterior border of *hoxd12a* expression (arrowhead) coincides with a lower segmental count in *hes6* mutant compared to wild-type embryos. The scale bar represents 0.3 mm. See also Figure S2, Table S2, and Table S3.

authors have suggested a counting mechanism, where the number of segmentation clock oscillations has an instructive role in positioning the anterior boundary of *Hox* gene expression and determining axial identity of segments [3, 4]. However, there is also evidence that *Hox* gene expression boundaries and axial identity of segments are at least partially specified prior to the ingression of cells into the PSM [19, 20], which would be inconsistent with a counting mechanism. We reasoned that the specifically slowed segmentation clock in the *hes6* mutant would provide independent evidence for one of these models and thus investigated the determination of axial identity in the mutant. We first examined the anterior border of *hoxd12a* expression [21] and found it at a lower segment number in *hes6* mutants compared to wild-type embryos (Figure 3C and Table 1). Again, this assay was done by an observer blind to the embryo's genotype, which was only determined after phenotypic analysis. This finding argues against an instructive role of the number of segmentation clock oscillations for placing this expression boundary.

Next, we assessed the alignment of anatomical structures with the file of segments. The proctodeum, marked by *evx1* expression, aligned with a lower segment count in *hes6* mutants compared to wild-type embryos (Figure 3A, arrowhead, and Table 1). We ruled out the possibility that this reflected a posterior shift of the whole file of paraxial mesoderm within the body by determining the segmental position of the anteriorly located pectoral fin bud in embryos costained for *tbx5* and *cb1045* expression. This structure was found at the level of the second segment both in wild-type and in *hes6* mutant embryos (Figure S2, Table S3). Finally, we looked

at anatomical markers in adult fish and asked whether they were associated with the same or a different number of segments in wild-type versus *hes6* mutant fish. Examination of rib number revealed that adult *hes6* mutants always had nine rib-bearing vertebrae whereas wild-type fish had nine or ten (Figure 3B and Table 1). Furthermore, the anterior insertion sites of the dorsal and anal fins were found to align with a lower segment count in the mutant fish compared to the wild-type (Figure 3B, arrowheads, and Table 1). In summary, all posterior axial markers examined here align with a lower segment number in *hes6* mutants compared to the wild-type. It therefore appears that the reduction in segment number in the *hes6* mutant is equally distributed to the different parts of the axis (trunk and tail), and it suggests that the specification of axial identity occurs independent of the number of segments or segmentation clock oscillations. Thus, we find no evidence for a regulatory link between the dynamics of the segmentation clock and the specification of axial regional identity. Instead, our results indicate that these two developmental modules can be dissociated through mutation of a single gene involved in the clock mechanism.

Homeotic transformations, e.g., through the mutation of *Hox* genes [22, 23], are changes in the specification of axial identity that occur independently of segment number and body growth. Furthermore, phylogenetic studies have established that region-specific changes in segment number and *Hox* gene expression have occurred several times during evolution [13, 24–26]. Together with the results presented in this report, these findings support the idea that the developmental modules that specify segment number and those that

determine their region-specific differentiation are largely independent and dissociable. This dissociability has probably been advantageous in evolution, because it facilitates the exploration of novel body plans.

Conclusions

In this report we use a zebrafish mutant with a slowed segmentation clock to investigate the role of this developmental module in the specification of segment number and the determination of axial regional identity. We confirm a central prediction of the original Clock and Wavefront model by showing that this slowed clock in a normally elongating axis leads to a reduction in segment number. Furthermore, we find that the reduction in segment number is evenly distributed across different axial regions. Taken together, these data show that through the mutation of a single gene, the dynamics of the segmentation clock can be dissociated from the developmental modules that govern axial elongation and determine regional identity. This finding complements extensive previous work on *Hox* gene mutants, which showed how axial regionalization could be experimentally dissociated from segmentation and axial outgrowth [18]. What now remains to be tested is whether axial outgrowth can be manipulated without affecting clock period and regionalization. Although this test may be more difficult, because of the pleiotropic effects of the signaling pathways involved [15], it supplies the missing link in understanding the interplay of growth, segmentation, and regionalization that shapes the vertebrate axial body plan in development and evolution.

Supplemental Information

Supplemental Information includes two figures, three tables, Supplemental Experimental Procedures, and one movie and can be found with this article online at doi:10.1016/j.cub.2010.05.071.

Acknowledgments

We are grateful to C.P. Heisenberg, S. Grill, J. Gibson-Brown, A. Ward, R. Ho, J. Cooke, and all members of the Oates lab for insightful discussions and helpful comments on various versions of this manuscript. We acknowledge the Max Planck Institute of Molecular Cell Biology and Genetics (MPI-CBG) sequencing facility, the fish facility, and the light microscopy facility for their excellent support. This work was supported by the Max Planck Society and by the European Research Council under the European Communities Seventh Framework Programme (FP7/2007-2013) / ERC Grant no. 207634.

Received: March 2, 2010

Revised: May 3, 2010

Accepted: May 4, 2010

Published online: July 15, 2010

References

1. Cooke, J., and Zeeman, E.C. (1976). A clock and wavefront model for control of the number of repeated structures during animal morphogenesis. *J. Theor. Biol.* 58, 455–476.
2. Cooke, J. (1981). The problem of periodic patterns in embryos. *Philos. Trans. R. Soc. Lond. B Biol. Sci.* 295, 509–524.
3. Dubrulle, J., McGrew, M.J., and Pourquié, O. (2001). FGF signaling controls somite boundary position and regulates segmentation clock control of spatiotemporal Hox gene activation. *Cell* 106, 219–232.
4. Jouve, C., Imura, T., and Pourquié, O. (2002). Onset of the segmentation clock in the chick embryo: Evidence for oscillations in the somite precursors in the primitive streak. *Development* 129, 1107–1117.
5. Holley, S.A. (2007). The genetics and embryology of zebrafish metamorphism. *Dev. Dyn.* 236, 1422–1449.
6. Kawamura, A., Koshida, S., Hijikata, H., Sakaguchi, T., Kondoh, H., and Takada, S. (2005). Zebrafish hairy/enhancer of split protein links FGF signaling to cyclic gene expression in the periodic segmentation of somites. *Genes Dev.* 19, 1156–1161.
7. Amsterdam, A., Burgess, S., Golling, G., Chen, W., Sun, Z., Townsend, K., Farrington, S., Haldi, M., and Hopkins, N. (1999). A large-scale insertional mutagenesis screen in zebrafish. *Genes Dev.* 13, 2713–2724.
8. Sieger, D., Ackermann, B., Winkler, C., Tautz, D., and Gajewski, M. (2006). *her1* and *her13.2* are jointly required for somitic border specification along the entire axis of the fish embryo. *Dev. Biol.* 293, 242–251.
9. Schröter, C., Herrgen, L., Cardona, A., Brouhard, G.J., Feldman, B., and Oates, A.C. (2008). Dynamics of zebrafish somitogenesis. *Dev. Dyn.* 237, 545–553.
10. Needham, J. (1933). On the dissociability of the fundamental processes in ontogenesis. *Biol. Rev. Camb. Philos. Soc.* 8, 180–223.
11. Raff, R.A. (1996). *The Shape of Life: Genes, Development, and the Evolution of Animal Form* (Chicago: The University of Chicago Press).
12. Richardson, M.K., Allen, S.P., Wright, G.M., Raynaud, A., and Hanken, J. (1998). Somite number and vertebrate evolution. *Development* 125, 151–160.
13. Ward, A.B., and Braender, E.L. (2007). Evolution of axial patterning in elongate fishes. *Biol. J. Linn. Soc. Lond.* 90, 97–116.
14. Gomez, C., Ozbudak, E.M., Wunderlich, J., Baumann, D., Lewis, J., and Pourquié, O. (2008). Control of segment number in vertebrate embryos. *Nature* 454, 335–339.
15. Wilson, V., Olivera-Martinez, I., and Storey, K.G. (2009). Stem cells, signals and vertebrate body axis extension. *Development* 136, 1591–1604.
16. Bae, S., Bessho, Y., Hojo, M., and Kageyama, R. (2000). The bHLH gene *Hes6*, an inhibitor of *Hes1*, promotes neuronal differentiation. *Development* 127, 2933–2943.
17. Lewis, J. (2003). Autoinhibition with transcriptional delay: A simple mechanism for the zebrafish somitogenesis oscillator. *Curr. Biol.* 13, 1398–1408.
18. Wellik, D.M. (2007). Hox patterning of the vertebrate axial skeleton. *Dev. Dyn.* 236, 2454–2463.
19. Imura, T., and Pourquié, O. (2006). Collinear activation of *Hoxb* genes during gastrulation is linked to mesoderm cell ingression. *Nature* 442, 568–571.
20. Szeto, D.P., and Kimelman, D. (2006). The regulation of mesodermal progenitor cell commitment to somitogenesis subdivides the zebrafish body musculature into distinct domains. *Genes Dev.* 20, 1923–1932.
21. van der Hoeven, F., Sordino, P., Fraudeau, N., Izpisua-Belmonte, J.C., and Duboule, D. (1996). Teleost *HoxD* and *HoxA* genes: Comparison with tetrapods and functional evolution of the HOXD complex. *Mech. Dev.* 54, 9–21.
22. Horan, G.S., Ramirez-Solis, R., Featherstone, M.S., Wolgemuth, D.J., Bradley, A., and Behringer, R.R. (1995). Compound mutants for the paralogous *hoxa-4*, *hoxb-4*, and *hoxd-4* genes show more complete homeotic transformations and a dose-dependent increase in the number of vertebrae transformed. *Genes Dev.* 9, 1667–1677.
23. Le Mouellic, H., Lallemand, Y., and Brûlet, P. (1992). Homeosis in the mouse induced by a null mutation in the *Hox-3.1* gene. *Cell* 69, 251–264.
24. Burke, A.C., Nelson, C.E., Morgan, B.A., and Tabin, C. (1995). Hox genes and the evolution of vertebrate axial morphology. *Development* 121, 333–346.
25. Müller, J., Scheyer, T.M., Head, J.J., Barrett, P.M., Werneburg, I., Ericson, P.G., Pol, D., and Sánchez-Villagra, M.R. (2010). Homeotic effects, somitogenesis and the evolution of vertebral numbers in recent and fossil amniotes. *Proc. Natl. Acad. Sci. USA* 107, 2118–2123.
26. Polly, D.P. (2001). Testing modularity and dissociation: The evolution of regional proportions in snakes. In *Beyond Heterochrony: The Evolution of Development*, M.L. Zelditch, ed. (New York: Wiley-Liss), pp. 305–336.